GEOTHERMAL CORROSION AND CORROSION PRODUCTS

Keith A. Lichti, Selo Soylemezoglu,
and Kevin D. Cunliffe

Industrial Processing Division
Department of Scientific and Industrial Research
New Zealand

ABSTRACT

The corrosion of carbon steels in geothermal fluids containing significant concentrations of H_2S and CO_2 often results in formation of thick, adherent layers of corrosion products. These films are essential to the corrosion resistance of carbon steel yet they also contribute to heat exchanger fouling, valve fouling and orifice restrictions.

Carbon steel and low alloy steel corrosion rates are reported for bore fluid (two phase), separated water, separated steam, and wet steam derived from the geothermal field at Broadlands, New Zealand. Methods are described which permit calculations of corrosion product thickness from material loss determinations obtained using flat coupons and cylindrical Corrosometer probes. Corrosion rates and estimated corrosion product formation rates are compared and discussed, with reference to pitting propensity and corrosion product adhesion. Differences in corrosion performance of differing corrosion monitors are explained.

INTRODUCTION

Corrosion of carbon steel in geothermal steam at Broadlands results in formation of the iron sulphides mackinawite, troilite and pyrrhotite. The overall corrosion reaction is of the form:

$$(1 \pm x)\ Fe + H_2S \rightarrow Fe_{(1 \pm x)}S + H_2 \qquad (1)$$

Techniques for obtaining carbon steel corrosion rates using hydrogen probes, Corrosometer* probes and coupons were outlined by McAdam et al., 1981, who demonstrated that comparable mean corrosion rates were obtained with all these monitors during short term (up to 6 weeks) exposures in unaerated geothermal fluids. This paper deals primarily with the results of longer term exposures of Corrosometer probes and coupons of up to one year.

Metal coupons of carbon steel when exposed to geothermal fluids often show an increase in weight due to formation of iron sulphide corrosion products. Removal of these products gives a weight loss, due to corrosion, from which corrosion rates are obtained. Weight gain results can however be used to predict corrosion rates or corrosion product thicknesses which can be related to observations of corrosion product adhesion, secondary corrosion product formation and pitting corrosion. In some cases, the thickness of corrosion products can be used to estimate corrosion rates based on a knowledge of corrosion mechanism and corrosion product composition. Applications where corrosion product formation rates are of interest include studies of heat exchanger fouling and estimation of historic corrosion rates.

DESCRIPTION OF EXPERIMENTS

Exposures of carbon and low alloy steel corrosion monitors having chemical composition as given in Table 1 were conducted in the Broadlands geothermal fluids derived from bore BR22. Results are reported for tests in bore fluid, separated water, separated steam and wet low pressure steam. The physical conditions, of exposure are detailed in Table 2. Table 3 describes the chemistry of the test fluids (Glover, 1980). Insulated metal coupons of the type described in ASTM standards G1-72 and *G4-68* which provide weight gain as well as weight loss results were exposed in two series of tests conducted in 1976/77 and 1978/79. Both tests included three distinct exposure periods of *4*, 13 and 52 weeks. During the second series, cylindrical carbon steel Corrosometer probes which give a daily measure of corrosion were simultaneously exposed via access ports in the tops of the test vessels as detailed in Figure 1. Corrosometer probes were electrically isolated from the carbon steel test vessel.

Soylemezoglu, S. et al., 1980, and McAdam, G.D., et al., 1981, have described the operating principles of the electrical resistance type Corrosometer probes used for this work. Braithwaite and Lichti, 1981, detail the methods of material preparation and cleaning which were used. Corrosion products were identified by X-ray diffractometry and pit densities and depths were determined using the methods outlined in ASTM standard G46-76. Weight loss (after removal of corrosion products) data were used to calculate material losses and corrosion rates. Weight loss, weight gain (after corrosion) and weight of corrosion products were used to estimate the thickness of corrosionproducts.

CORROSION CALCULATIONS

The material lost ML(Fe) by corrosion of a

* Magna Instruments (Rohrback Corp.) USA

TABLE 1. CHEMICAL COMPOSITION OF CORROSION MONITORS

Monitor Material	Type AISI Designation	Composition (Element weight percent). C	Mn	Si	Ni	Cr	Mo	cu
Coupons								
Carbon Steel*	1018	0.15–0.19	0.62	<0.02	0.03	0.04	<0.03	<0.01
Alloy Steel**	4140	0.41	0.82	0.28	0.21	0.87	0.19	0.22
Corrosometer								
Carbon Steel	1010	0.06	0.45	0.10	0.14	0.10	0.04	0.17

*Manufactured from flat plate. **Manufactured from rod.

TABLE 2. PHYSICAL CONDITIONS OF EXPOSURE

Environment (Air–free)	Pressure (kPa)	Temperature (°C)	Mass flow ($kg\ h^{-1}$)	Fluid velocity ($m\ h^{-1}$)	Remarks
Bore fluid	650	160	178	87	Two–phase fluid
Separated water	650	160	56	1.2	Liquid
Separated steam	650	160	40	70	Dry steam
Wet steam	126	105	57	1.3×10^{3}	10%wet steam

TABLE 3. CHEMICAL CONDITIONS OF EXPOSURE

Environment (Air–free)	a: Gas–phase partial pressure (kPa) CO_2	H_2S	NH_3	N_2	CH_4	H_2
Bore, fluid	6.50	1.33×10^{-1}	2.54×10^{-2}	4.05×10^{-2}	8.26×10^{-2}	6.45×10^{-3}
Separated steam	5.53	1.23×10^{-1}	2.69×10^{-2}	5.14×10^{-2}	6.83×10^{-2}	5.23×10^{-3}
Wet steam	1.07	2.10×10^{-2}	4.61×10^{-3}	1.17×10^{-2}	1.14×10^{-2}	8.49×10^{-4}

	b: Calculated water–phase chemistry at test conditions ($mg\ kg^{-1}$) pH	CO_2	HCO_3^-	H_2S	HS^-	NH_3	NH_4^+
Bore fluid	7.4	26.5	137.	1.6	5.50	4.7	0.43
Separated water	7.4	29.4	158.	1.8	6.9	4.4	0.62
Separated steam	6.5	20.6	11.1	1.3	0.48	4.2	3.6
Wet steam	6.9	5.0	22.	0.27	0.52	2.6	7.0

c: Water–phase chemical analyses at ambient* temperature and pressure ($mg\ kg^{-1}$)

	pH	K($S\ m^{-1}$)	Fe	SO_4^{2-}	Si02	Cl^-	B	F^-
Bore fluid (water only)	7.8	0.48	0.3	10	706	1410	?	?
Separated water	7.9	-0.5	?	7	727	1436	39.1	5.3
Separated steam	5.5	0.042	1.6	<1	2	-	-	-
Wet steam	5.2	0.021	-	<1	<1	-	-	-

* About 20°C and 100 kPa.

flat coupon can be calculated from the equation:

$$ML(Fe) = \delta(Fe)/(\rho(Fe))A \qquad (2)$$

where $\delta(Fe)$ is the weight of iron lost by corrosion, $\rho(Fe)$ is the density of iron and A is the exposed surface area of the coupon.

Three methods are available to calculate corrosion product thickness (described as material gain, MG(FeS)) for the flat coupons. In all cases the calculations are made for formation of troilite (FeS) only and the hydrogen is assumed lost. Firstly the ratio of the molar volumes of FeS to Fe is proportional to the ratio of thickness of FeS formed to Fe used in reaction 1. Therefore from reaction 1:

$$MG(FeS) \simeq 2.61\ ML(Fe) \qquad (3)$$

Seccndly, the weight change occurring on exposure can be attributed to absorption of sulphur and the ratio of molecular weight of FeS to that of S is proportional to the ratio of weights of FeS and S involved.

Again from reaction (1):

$$\delta(FeS) \simeq 2.74\delta(S) \qquad (4)$$

where $\delta(FeS)$ is the calculated weight of FeS formed and $\delta(S)$ is the weight gained during the exposure. MG(FeS) is calculated from $\delta(FeS)$ and $\rho(FeS)$, the density of FeS, using an equation of the same form as (2). Thirdly the actual weight of FeS formed can be determined from:

$$\delta(FeS) \simeq \delta(Fe) + \delta(S) \qquad (5)$$

and MG(FeS) calculated as outlined above.

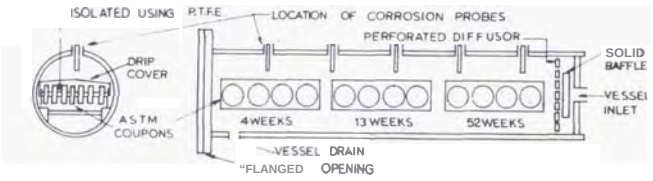

Figure 1: Location of coupons and Corrosometer probes in steam test vessels.

All of these calculations assume that the corrosion products are dense, non porous, that none of the corrosion products are lost, and that none of the hydrogen is retained in the steel. Small errors in the order of 5 to 10% arise in using the data for troilite when mackinawite and pyrrhotite may also be present.

For Corrosometer probes only the first method using equation (3) is feasible. The material loss is first obtained from Corrosometer dial readings. The instrument has a maximum of 1000 dial readings which are equivalent to half the probe thickness, or 127 μm (0.005 inch) for a probe with a 254 μm (0.010 inch) wall thickness. The calculated ML(Fe) is then substituted into equation (3) to give MG(FeS).

RESULTS

Material loss results for the carbon steels are summarised in Figures 2,3 and 4 for bore fluid, separated steam and wet low pressure steam respectively. Table 4 lists discrete values of material loss, material gain, observed pitting propensity, identified corrosion products and silicon content of typical scales formed on carbon steel racks (which held the exposed coupons) and on the Corrosometer probes.

Corrosion monitoring in separated water was limited to coupons exposed in the 1976/77 series of exposures. All ferrous alloys were coated by a layer of amorphous silica which deposited at a near linear rate of ~60 $\mu m y^{-1}$. Carbon and low alloy steels were corroded to a depth of 0.27 μm in the one year exposure however pits having a maximum depth of 25 μm (after 4 weeks) were observed in the region covered by the PTFE spacers. Small amounts of corrosion product were collected and were identified as a mixture of troilite and mackinawite.

DISCUSSION

Different corrosion results obtained for Corrosometer probes and coupons in seemingly identical conditions can be explained on the basis of differences in the experimental parameters. The cylindrical carbon steel Corrosometers have a radius of 3,25mm while coupons have essentially infinitely flat surfaces. This difference is referred to as the shape factor. Corrosometer probes were located at the top of the vessel whereas coupons were at the half way position in the 254mm (10 inch) diameter test vessel. Short term coupon exposures were at the front of the test vessel and long term at the rear, near the fluid inlet. These differences are referred to as location factors. In addition, the long term exposures were subjected to repeated vessel openings and other unavoidable temporary changes in physical and chemical conditions, These variations are described as exposure factors. Other parameters such as material differences which also influence the results are discussed in detail.

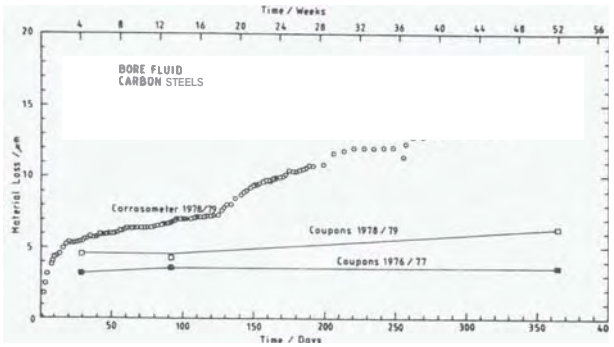

Figure 2: Material loss results for carbon steel corrosion monitors exposed to bore fluid.

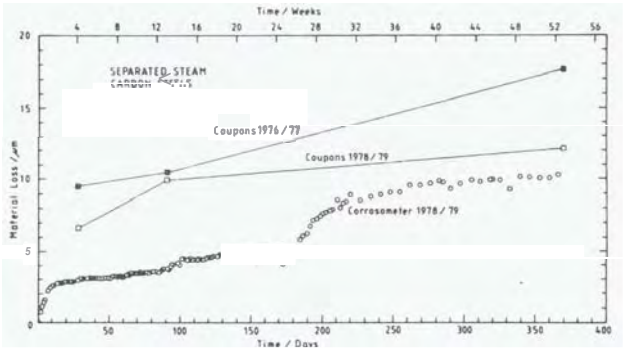

Figure 3: Material loss results for carbon steel corrosion monitors exposed to separated steam.

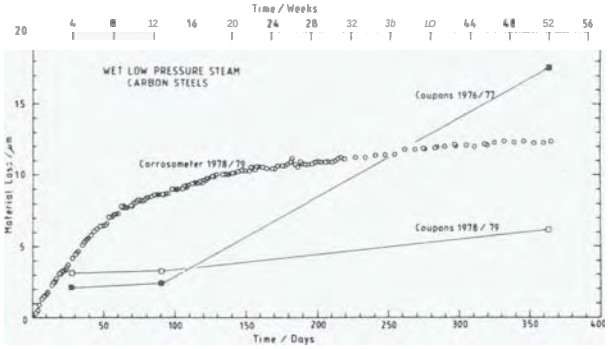

Figure 4: Material loss results for carbon steel corrosion monitors exposed to wet low pressure steam.

Material gain calculated from material loss (weight of iron lost δ(Fe) in Table 4) gives an idealised value of corrosion product thickness. If the formed product is troilite and none is lost then the material gain obtained from δ(S) or δ(FeS) or both will agree with the idealised value. If the

TABLE 4: CARBON AND LOW ALLOY STEEL CORROSION RESULTS.

Environment / Material Type / Exposure Period	Exposure Time	ML δ(Fe)	MG δ(Fe)	MG δ(S)	MG δ(FeS)	Pitting Density	Pit Depths On Face avg*(max)	Pit Depths Under PTFE avg*(max)	Corrosion Products by X-Ray	Integrity	Silicon
	Weeks	µm	µm	µm	µm	G46-76	µm(µm)	µm(µm)			wt%
Bore Fluid											
Carbon Steel 1978/79	4	4.76	12.4	10.3	11.6	4	18(29)	24(58)		A	0.15
	13	4.28	11.2	10.3	10.8	5	20(33)	21(36)		A	0.30
	52	6.33	16.5	16.8	17.1	5+	24(84)	36(61)		A	0.45
Corrosometer	52	14.3	37.3	-	-	5+	20(53)	-	T+{U+AU}	A	0.08
Carbon Steel 1976/77	4	3.23	8.43	7.54	8.20	3	8(13)	9(20)	T	A	0.15
	13	3.54	9.23	9.66	9.28	4	7(11)	16(30)	T	A	0.30
	52	3.59	9.37	12.5	10.5	5	7(11)	30(49)	T+{U}	A	0.45
Low Alloy Steel 1976/77	4	2.90	7.60	3.81	6.16	4	<5(10)	9(18)	-	A/F	-
	13	3.45	9.01	loss	5.01	5	<5(10)	17(32)	T	A/F	-
	52	2.00	5.22	7.06	5.82	5	10(20)	17(36)	T+P	A/F	-
Separated Steam											
Carbon Steel 1978/79	4	6.67	17.4	14.4	16.6	5+	24(46)	17(56)	T+{Mac+U}	A	0.09
	13	9.95	26.0	22.0	24.7	5+	25(44)	17(62)	T	A	0.05
	52	12.2	31.8	29.1	30.4	5+	22(37)	18(45)	Pyrr+{U}	A	0.15
Corrosometer	52	10.4	27.1	-	-	5+	16(37)	-	T+{U+AU}	A	0.02
Carbon Steel 1976/77	4	9.52	24.9	17.0	21.9	3	24(45)	12(19)	Mac+{Pyrr}	A	0.09
	13	10.5	27.3	24.7	26.3	3	22(44)	12(23)	Mac+Pyrr	A	0.15
	52	17.7	46.2	43.3	44.9	5+	98(178)	16(29)	Pyrr+Mac	F	0.09
Low Alloy Steel 1976/77	4	6.20	16.2	10.4	13.9	5	11(18)	11(27)	Mac+Pyrr+T+U	A	
	13	9.23	24.1	loss	16.7	5	13(21)	13(24)	Mac+Pyrr+T+U	F	
	52	31.0	80.9	loss	34.0	5+	50(79)	28(56)	T	F	
Wet Low Pressure Steam											
Carbon Steel 1978/79	4	3.14	8.20	5.73	7.03	3	7(20)	8(14)	Mac+U	A	0.015
	13	3.27	8.54	8.25	8.47	5+	11(20)	13(21)	Mac+{P+Pyrr+U}	A	0.015
	52	6.14	16.0	15.2	15.3	5+	34(73)	13(28)	P+Pyrr	A	0.06
Corrosometer	52	12.5	32.6	-	-	5+	19(30)**	-	T+Mac+{U+AU}	A/F	0.06
Carbon Steel 1976/77	4	2.12	5.53	4.84	5.13	<1	<5(10)	<5(9)	Mac+U	A	
	13	2.41	6.29	6.36	6.29	<1	<5(14)	10(16)	Mac+T	A	-
	52	17.6	45.8	46.2	45.8	5+	36(74)	16(30)	***	F	****
Low Alloy Steel 1976/77	4	1.56	4.07	3.75	3.95	<1	15(22)	18(26)	-	A/F	
	13	2.10	5.48	5.53	5.49	<1	6(11)	6(13)	Mac+Pyrr+T	A	
	52	23.5	61.4	59.7	59.9	5+	50(79)	30(74)	Pyrr+T+iron	F	

P = Pyrite FeS_2
Pyrr = Pyrrhotite $Fe_{(1-x)}S$
T = Troilite FeS
Mac = Mackinawite $Fe_{(1+x)}S$
S = Sulphur S
Mgn = Magnetite Fe_3O_4

U = Unknown
AU = Amorphous Unknown
{} = Minor Components
A = Adherent Corrosion Products
F = Flaking Corrosion Products
A/F = Non Uniform Adhesion

*Average of >40 readings/exposure period. Pits showing the greatest depth were selected for measurement.
** Corrosion Band 0.127 mm deep x 2.5 mm wide x 20 mm long.
*** Mac+T+P+Mgn+S+$FeSO_4 \cdot H_2O$
**** Test Vessel Corrosion Products = 0.06 wt%Si

results from δ(S) and δ(FeS) are less than ideal then corrosion product loss into solution or by flaking is likely to have occurred., and the degree of variation may reveal the extent of the loss. If the results are higher than ideal, then the assumption that ,the corrosion products are essentially troilite may be in error.

BORE FLUID

In bore fluid (see Figure 2) protective films of troilite formed and corrosion decreased to low levels by 4 weeks. The Corrosometer probe however gave higher corrosion rates than the carbon steel coupons. Of the 9 easily detected discontinuities in the Corrosometer results, 7 were attributable to known vessel openings and ingress of air,

although 4 vessel openings had no apparent effect. Table 4 gives details of the general stability of troilite on the carbon steel and shows that on the low alloy steel extensive corrosion product flaking occurred. Material gain results reflect this good adhesion on carbon steels and the onset of flaking from the alloy steel. The MG based on $\delta(S)$ and $\delta(FeS)$ are lower than the ideal given by MG based on $\delta(Fe)$ in Table 4. The 52 week corrosion results for the alloy steels were anomolously low, possibly due to the formation of pyrite. Pitting was most severe during the 1978/79 exposures. The corrosion products on the Corrosometer probe were low in silicon and those on the carbon steel racks, which held the coupons in place, had higher silicon levels reducing to a value of 0.15 wt% at the front of the test vessel.

Glover, 1979, demonstrated that the experimental test vessel acted as a horizontal separator and the dissolved solids and ammonia tended to partition into the water phase. The water droplet content of the "two phase fluid" reduced toward the top and front of the vessel. The detected silicon distribution reflected this water separation, and it was assumed that the Cl^- ions also followed this distribution.

The difference in the corrosion results are attributed to exposure factors which affect monitors in different ways because of their location. The discontinuities in the Corrosometer results seen in Figure 2 suggest a pitting (due to oxygen or chloride ion, Shrier, 1976) or a film crack and heal mechanism (due to thermal stresses, Uhlig, 1948), or both, which are not evident in the coupon results. Silicon levels in the scales (Table 4) and the assumed water distribution in the vessel correlate well with the material loss and gain results. The Corrosometer probe which was located in the upper portion of the vessel was exposed to unbuffered steam condensate. This probe gave the highest material loss result, was sensitive to vessel openings and may also have been effected by the shape factor.

The coupons which were in the lower portion of the test vessel gave lower corrosion rates because of the buffering effect of ammonia and the corrosion inhibiting properties of silica. The coupons were also less effected by vessel openings in spite of the assumed presence of chloride ions.

SEPARATED STEAM

Corrosion in this environment also decreased to a low level by 4 weeks (Figure 3). The Corrosometer which had stable films consisting mainly of troilite gave lower results than the coupons which often formed mackinawite and pyrrhotite. (see Table 4). 15 Corrosometer discontinuities were readily evident and 9 of those including the one at 170 days corresponded to known vessel openings. 3 vessel openings had no apparent effect. In this environment the highest silicon levels in the formed corrosion products were again recorded on the coupon racks. All of the carbon steels had good corrosion product adhesion while a significant loss of corrosion products occurred from the low alloy steel. Pitting was most severe on the carbon steel coupons exposed in 1976/77, and material loss and material gain results parallel this effect. A high but more uniform material loss result was observed for the 52 week exposure of the alloy steel again presumed to be due to poor adhesion of the corrosion products. Material gain. calculated from weight of corrosion products was noticably low, reflecting the loss of corrosion product adhesion, on the low alloy steels.

Separator water droplet carryover and steam condensation contributed small amounts of moisture to separated steam. The amount and chemical composition of the liquid which forms on the corrosion monitors determines the corrosion rates. If gravity separation gave a moisture distribution similar to that of the bore fluid vessel, then the coupons in the lower portion of the test vessel would have had more liquid adhearing to them. The higher coupon corrosion rates (see Figure 3 and Table 4) are attributed to this assumed moisture distribution. In this environment silicon levels were generally low and did not correlate with corrosion rates or corrosion product adhesion. The coupons show some sensitivity to vessel openings but the effects are obscure because of the limited number of exposures. Figure 3 shows that the Corrosometer probe reflects the effect of vessel openings more than the coupons. The opening at 170 days (an extended probe port opening) caused a doubling of the observed material loss bringing the Corrosometer and coupon corrosion rates and pit depths to similar values. With the available evidence it is impossible to attribute this Corrosometer probe discontinuity to a single mechanism since film cracking due to thermal stress or pitting due to oxygen could both have caused the observed effect. The lack of change in the coupon response over this time period does lend support to a film cracking mechanism, the difference in performance being due to the shape factor.

WET LOW PRESSURE STEAM

The 1976/77 coupon results were characterised by a sharp increase in material loss at some time after the 13 week expsoure (Figure 4 and Table 4). This has been attributed to the onset of pitting corrosion caused by oxygen ingress at vessel openings and was evidenced by formation cf thick, poorly adherent corrosion products which contained free sulphur and hydrated ferrous sulphate (Braithwaite and Lichti, 1981). Flaking of the corrosion products was noted; however, material gain calculations did not reflect significant loss of corrosion products or large changes in composition.

In the 1978/79 series of tests the coupons were less effected by known vessel openings and had good corrosion product adhesion. The Corrosometer probe results suggested uniform protective film formation, even though 9 discontinuities were evident. 4 of these were attributed to vessel openings and an additional 4 openings had no apparent effect. However, after 52 weeks the Corrosometer corrosion products were distinctly non-uniform in appearance. A meandering band of porous and flaking corrosion products which appeared to have formed as a result of condensate

running down the side of the probe was readily evident. The remainder of the corrosion products mere dense and adherent.

It was thought that the complex fitting used to provide electrical isolation of the probe in the pressurised vessel had a high rate of heat transfer and caused formation of corrosive condensate at the top of the probe which drained along the sensing element. On removal of the corrosion products a corresponding band of pitting corrosion was exposed. In several regions the pitting was characterised by complete loss of material across the full width of the band giving a flat bottom area ≈2.5mm in width, having a maximum depth of ≈0.127mm and up to 20mm in length. Localised loss of this material from the electrical resistance type sense element would result in the Corrosometer recording a material loss of ≈6 μm. This figure corresponds to the 6 μm difference recorded between the coupons and the Corrosometer probe for the simultaneous exposures, implying that without this band of condensate corrosion, identical results would have been obtained. For this environment the observed corrosion performance characteristics were therefore determined by exposure factors resulting from experimental design and execution.

SEPARATED WATER

Broadlands bore BR22 contains 747 $mgkg^{-1}$ silica. The physical conditions selected to perform the steam/water separation (6.6 ba, ≈163°C) and separated water corrosion tests (6.5 ba, ≈160°C) gave a silica supersaturation ratio of >1.05 (Henley, 1981). The observed silica deposition caused by the supersaturation dominated the corrosion reactions occurring on all the ferrous alloys. The silica appeared to provide a uniform diffusion barrier to potentially corrosive species in the water. However, corrosion pits having a maximum depth of 25 μm were formed before the silica barrier was established. Corrosion mechanisms in this environment were therefore controlled by exposure factors resulting from experimental design and fluid chemistry.

CONCLUSIONS AND RECOMMENDATIONS

Carbon steel and low alloy steel (AISI 4140) exhibit low yearly corrosion rates (3 to 30 $\mu m y^{-1}$) iin geothermal bore fluid and steam. Corrosion product films consisting mainly of the iron sulphides, mackinawite, troilite and pyrrhotite were formed and their growth was directly related to the rate of corrosion. The ability of these protective films to reduce corrosion to a low level was enhanced by the presence of minute amounts of silicon in the scales, but was reduced when the test vessels were opened during the course of the experiments. Pitting corrosion occurred in all environments even when corrosion products were adherent. Measured pit depths were often >10 times deeper than average depths of corrosion. Silica deposition from solution dominated corrosion reactions in the separated water test.

The major cause of the observed differences in mean corrosion rate, as determined by coupons and Corrosometer probes was the different location of the monitors within the test vessel. Because of this the monitors were subjected to differences in corrosion chemistry resulting from the design of the experiments and from difficulties encountered when multiple tests were conducted'in a single chamber. Corrosometer probes-were more sensitive to exposure variations, but this was due to their shape factor, location and frequency of measurement.

Despite these differences many of the corrosion parameters used to characterise the corrosion performance of carbon steels in geothermal fluids can be measured using both of these monitors. Extreme care must however be taken to locate and mount the selected corrosion monitors in the appropriate position in the process streams.

ACKNOWLEDGEMENTS

The authors wish to acknowledge the technical assistance of H. Bijnen and J. Garvitch of IPD, DSIR and R. Berezowski, M. Bowden and J. M. Turner of CD, DSIR.

REFERENCES

ASTM G1-72, 1978, Standard Recommended Practice for Preparing, Cleaning and Evaluating Corrosion Test Specimens, ASTM Standards Part 10.

ASTM G4-68, 1978, Standard Recommended Practice for Conducting Plant Corrosion Tests, ASTM Standards Part 10.

ASTM G46-76, 1978, Standard Recommended Practice for Examination and Evaluation of Pitting Corrosion, ASTM Standards Part 10.

Braithwaite, W.R. and Lichti, K.A., 1980. Surface Corrosion of Metals in Geothermal Fluids at Broadlands, New Zealand, Geothermal Scaling and Corrosion ASTM STP 717, pp81-112.

Glover, R.B., 1979, private communication.

Glover, R.B., 1980, Determination of the Chemistry of Some Geothermal Environments, DSIR Open File CD 118/12-RBG41, Unpublished Results.

Henley, R., 1981, Silica Scaling Rates for Ohaki Waste Waters - A Review of Field Data, DSIR Open File CD 30/555/3-RWH8, Unpublished Results.

McAdam, G.D., Lichti, K.A. and Soylemezoglu, S., 1981, Hydrogen in Steel Exposed to Geothermal Fluids, In Press, Geothermics.

Shrier., L.L., ed, 1976, Corrosion Vol. 1, Metal/Environment Reactions, Newnes-Butterworth, 2nd edition, ppl:150-1:162.

Soylemezoglu, S., Lichti, K.A. and Bijnen, H., 1980, Geothermal Corrosion Case Studies at Wairakei and Broadlands Geothermal Fields Using the 'Corrosometer' Method in Proceedings of The New Zealand Geothermal Workshop.

Uhlig, H.H. ed, 1948, The Corrosion Handbook, John Wiley & Sons, pp13.